Effects of the Super Bialkali Photocathode on the Performance Characteristics of a Position-Sensitive Depth-of-Interaction PET Detector Module

Juan José Vaquero, *Senior Member, IEEE,* José M. Udías, Samuel España and Manuel Desco

***Abstract*– Super Bialkali (SBA) and Ultra Bialkali (UBA) photocathodes are new technologies that improve the spectral response characteristics of position sensitive PMTs, boosting their quantum efficiency up to 35% and 43% (typ.) respectively [ref Hamamatsu]. Two SBA tubes were introduced into a production line of PET detectors mixed with the regular ones. The detectors were assembled on the same day and by the same operator using the standard factory protocols for detector mounting, calibration and testing. In this work we are reporting our evaluation of the achieved improvement by comparing the spatial and energy resolutions and the depth-of-interaction performance of a PET detector modules with DOI capabilities assembled using the regular and the SBA versions of the same PS-PMT. We conclude that the superior performance of the SBA tube may enable the use of arrays with a larger number of crystals of smaller footprint, thus improving the detector intrinsic spatial resolution without degrading the energy resolution or the phoswich discrimination capability.**

I. Introduction

Photomultipliers (PMT) convert the incident light photons produced by the crystal scintillator into electrons by means of a photoemission process that occurs in the photocathode. The efficiency of this process depends on several physical phenomena well described in [1]. In terms of scintillation counting the most relevant parameters are the spectral response and the quantum efficiency (QE), the latter defined as the number of photoelectrons emitted divided by the number of incident photons. This energy conversion is followed by an electron mutiplication that results on a charge pulse at the final anode. Since the photoelectron conversion represents the first step in the amplification chain, any improvement on the QE should benefit the resulting overall performance of the PMT.

Super Bialkali (SBA) and Ultra Bialkali (UBA) photocathodes are new technologies that improve the spectral response characteristics of position sensitive PMTs, boosting their quantum efficiency up to 35% and 43% (typ.) respectively [2].

In this work we are reporting our evaluation of this improvement by comparing the spatial and energy resolutions and the depth-of-interaction performance of a PET detector module with PET capabilities assembled using the regular and the SBA versions of the same PS-PMT.

II. Materials and Methods

A. Detector Modules

Two SBA tubes (Hamamatsu R8900-100-C12) were introduced into a production line of PET detectors mixed with the regular ones (Hamamatsu R8520-00-C12). The detectors were assembled on the same day and by the same operator using the standard factory protocols for detector mounting, calibration and testing. The module comprises two more parts: the above mentioned PS-PMT is coupled to a phoswich scintillator crystal array (LYSO and GSO) in which each phoswich element is packed into a 13 x 13 white vinyl crate covered at the entrance end with PTFE tape to enhance reflection of scintillation light onto the PSPMT photocathode [3]. Finally, electronic circuits for high voltage (HV) generation, amplification and timing, all of them integrated on a single PCB, are attached to the PMTs.

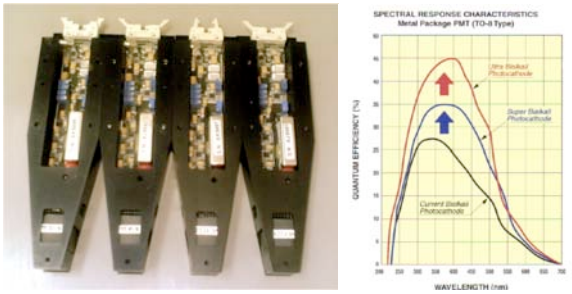

Fig. 1. Modules finished as they come out of the production line (left). QE curves for the regular, SBA and UBA PS-PMTs from Hamamatsu (right).

B. Data Acquisition and Processing

Data acquisition for all the detectors was done with the same equipment and settings: the 12 anode outputs (six for X and six for Y) are fed to a resistive divider that implement an Anger-like processing [4-6]; the resulting four signals that

Manuscript received November 4, 2008. This work was supported in part by the CENIT Programme (Ministerio de Industria), CIBER CB07/09/0031, RETIC-RECAVA (Ministerio de Sanidad y Consumo), and TEC2007-64731/TCM (Ministerio de Educación y Ciencia).

J.J. Vaquero and M. Desco are with the Unidad de Medicina y Cirugía Experimental, Hospital General Universitario Gregorio Marañón, Madrid, Spain (J.J. Vaquero email: juanjo@hggm es)

J.M. Udías and S. España are with the Grupo de Física Nuclear, Departamento de Física Atómica, Molecular y Nuclear, Universidad Complutense, Madrid, Spain.

locates the event within the field-of-view (FOV) are digitized using a charge-integration ADC. A delayed sum (energy) signal is also generated by summing the position signals and digitized it at the same time. LYSO and GSO events are discriminated from one another by applying the "delayed charge integration" technique, an algorithm based on the different light decay constants between the two scintillators to identify the scintillator of interaction [2].

The data acquisition protocol was identical for all the detectors: the lower threshold electronic cut-off was the same for both tubes, and there was no upper-level cut-off. Tube equalization was achieved by modulating the HV for each PMT. The images from the four detectors were analyzed to measure intrinsic module resolution, energy resolution and DOI performance using field flood images of a flat ^{68}Ge source and a ^{22}Na point source.

Intrinsic module resolution was quantified measuring peak-to-valley ratios and peak separation on different profiles across the PMTs field flood images [7].

Energy resolution was separately measured for each crystal by fitting a gaussian function to the photopeak, after discounting the scatter contribution. An ANOVA analysis was applied to all the crystals energy resolutions and the results were represented with a box-and-whisker plot. SBA tubes were tracked by their serial number and identified only at the end of the experiment.

The performance of the delayed charge integration depth – of-interaction (DOI) performance was measured by comparing the number of events correctly assigned to the phoswich elements.

III. Results

SBA PMT images in Fig. 2 (left) clearly show the "connect-the-dot" patterns described in [7], while they are more difficult to appreciate on the images from the regular PMTs (right). Fig. 3 depicts the central intensity profiles, and peak to valley ration and peak spacing are quantified in Table I.

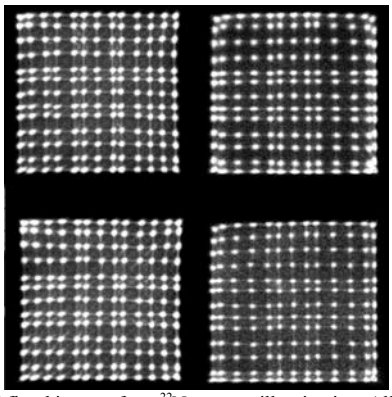

Fig. 2. Field flood images for a ^{22}Na source illumination. All images have been acquired with the same settings. Left column are the SBA tubes, right column the regular ones.

The crystal look-up table (LUT) resulting from the segmentation of a ^{68}Ge field flood illumination is shown in Fig. 4. The changes in size of regions of interest assigned to each crystal across the central row are depicted in the lower panel of the same figure.

TABLE I
PEAK SPACING ON THE CENTRAL PROFILE OF THE ^{68}GE FIELD FLOOD IMAGE (MEDIAN ± STD, IN PIXELS), AND PEAK-TO-VALLEY RATIO ON THE SAME PROFILE (MEDIAN ±STD)

tube	SBA	SBA	Reg.	Reg.
peak spacing	16.7 ±4.6	17.8 ±3.0	20.1 ±5.6	19.8 ±5.3
peak/valley	8.6 ±2.1	7.8 ±2 1	6 9 ±1.6	7.0 ±2.1

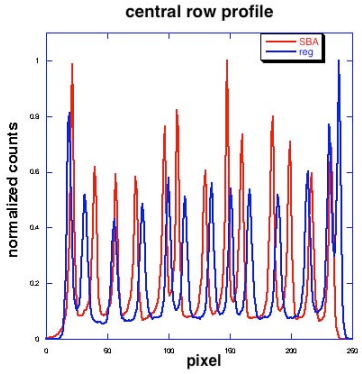

Fig. 3. Central row profile for a field flood illumination with ^{68}Ge.

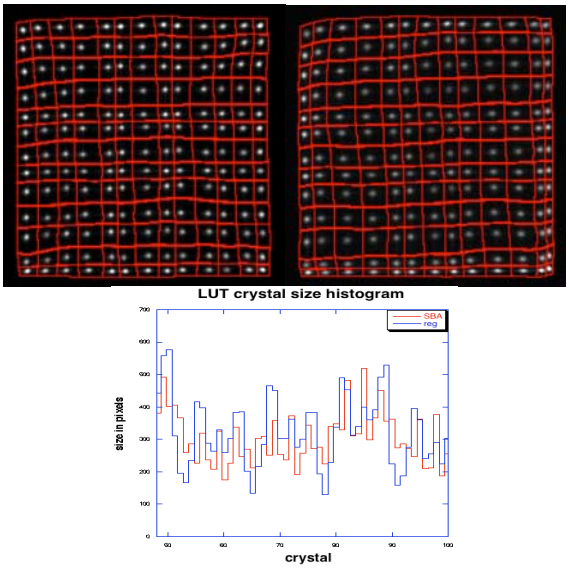

Fig. 4. Crystal LUT obtained from the ^{68}Ge field flood illumination; SBA tube on the left, regular tube on the right (upper panel). LUT crystal sizes histogram detail (lower panel).

The statistical results of energy resolutions measured for each crystal of each detector assembly are shown in Fig. 5. For each PMT, boxes representing the two intermediate quartiles of the FWHM in percentage are plotted. The whiskers represent the remaining two extreme quartiles, while the "+" and "o" symbols represent outliers.

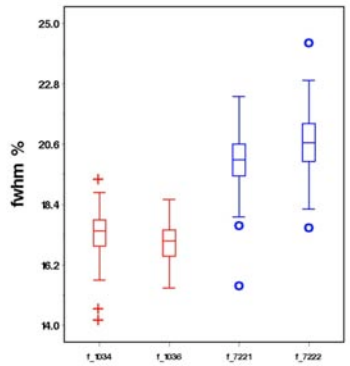

Fig. 5. Box and whisker plot for the individual LYSO crystals energy resolution, for a ^{68}Ge field flood illumination (SBA: red, reg.: blue). Statistical difference was significant ($p<0.0001$).

The result of the "delayed charge integration" method used to discriminate the phoswich crystals is presented in Fig. 6. The two shadows on each image represent the footprint of the rations between the total and delayed energy signals: the vertical axis is "energy" or "full charge" and the horizontal axis is the ratio "delayed charge"-to-"full charge", times a scale factor. The smaller ratio (vertical shaped blob on the left) corresponds to LYSO and the larger one (round shaped blob on the right) to GSO. Sharper blobs indicate better performance.

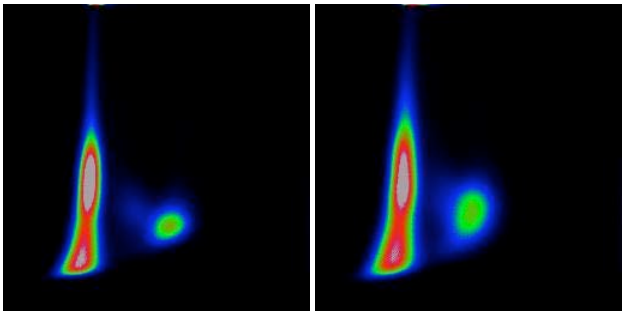

Fig. 6. Phoswich diagrams for the SBA tube (left) and the regular tube (right). Both images are shown using the same window/level normalized settings. SBA phoswich diagram is sharper than the regular one.

IV. Discussion and Conclusions

Fig. 2 shows that the SBA reveals more details in the field flood: the "connect-the-dot" patterns are clearly depicted. More evenly spaced crystals can also be appreciated on the SBA image and on the central row profile (Fig. 4). Profiles accross these central row profiles shows a better peak to valley ratio for the SBA tubes. This intrinsic spatial resolution improvement of the SBA can also be appreciated on the crystal LUT: the SBA tube produces more regular regions on the crystals LUT (upper panel in Fig. 4), reducing the apparent crystal sizes variability (lower panel, Fig. 4). Energy resolution improves significantly for the LYSO crystal with the use of the SBA photomultiplier (Fig. 5).

Using the same classification criteria to analyze the phoswich resolution, the SBA tubes show an improvement of 25% on number of events assigned to one of the crystals (Fig. 6).

We conclude that the superior performance of the SBA tube may enable the use of arrays with a larger number of crystals of smaller footprint, thus improving the detector intrinsic spatial resolution without degrading the energy resolution or the phoswich discrimination capability.

Acknowledgment

We thank SUINSA Medical Systems from providing part of the materials and tools used on this experiment.

References

[1] G. F. Knoll, "Radiation detection and measurement," John Wiley & Sons, Inc., 2000.

[2] K. K. Hamamatsu-Photonics, "Hamamatsu Super Bialkali Photocathodes," 2006.

[3] J. Seidel, J. J. Vaquero, S. Siegel, W. R. Gandler, and M. V. Green, "Depth Identification Accuracy of a Three-Layer Phoswich PET Detector Module," *IEEE Trans Nucl Sci,* vol. 46, pp. 485-490, 1999.

[4] S. Siegel, R. W. Silverman, Y. Shao, and S. R. Cherry, "Simple Charge Division Readouts for Imagine Scintillator Arrays using a Multi-Channel PMT," *IEEE Transactions on Nuclear Science,* vol. 43, pp. 1634-1641, June 1996 1996.

[5] V. Popov, S. Majewski, and A. G. Weisenberger, "Readout Electronics for Multianode Photomultiplier Tubes With Pad Matrix Anode Layout," *2003 IEEE Nuclear Science Symposium Conference Record,* vol. 3, pp. 2156 - 2159, 19-25 Oct. 2003 2003.

[6] V. Popov, S. Majewski, A. G. Weisenberger, and R. Wojcik, "Analog Readout System with Charge Division Type Output," *2001 IEEE Nuclear Science Symposium Conference Record,* vol. 4, pp. 1937-1940, 4-10 Nov. 2001.

[7] J. J. Vaquero, J. Seidel, S. Siegel, W. R. Gandler, and M. V. Green, "Performance Characteristics of a Compact Position-Sensitive LSO Detector Module," *IEEE Trans Med Imag,* vol. 17, pp. 967-978, 1998.